

Chiral Imidazolium Receptors for Citrate and Malate: The Importance of the Preorganization

Enrico Faggi,[†] Raúl Porcar,[‡] Michael Bolte,[§] Santiago V. Luis,[‡] Eduardo García-Verdugo,[‡] and Ignacio Alfonso^{*,†}

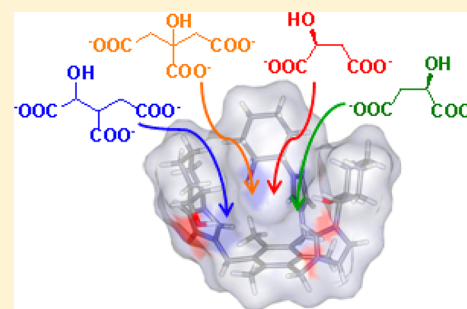
[†]Departamento de Química Biológica y Modelización Molecular, IQAC–CSIC, Jordi Girona, 16-26, E-08034 Barcelona, Spain

[‡]Departamento de Química Inorgánica y Orgánica, Universitat Jaume I, Av. de Vicent Sos Baynat s/n, E-12071 Castellón de la Plana, Spain

[§]Institut für Anorganische Chemie, J.-W.-Goethe-Universität, Max-von-Laue-Str.7, D-60438 Frankfurt/Main, Germany

Supporting Information

ABSTRACT: A family of simple receptors formed by two or three cationic imidazolium arms attached to a central aromatic linkage and displaying different conformational flexibility has been synthesized from the enantiopure (1*S*,2*S*)-2-(1-*H*-imidazol-1-yl)-cyclohexanol. The crystal structures of the corresponding bromides of two of the hosts showed remarkable differences. The tripodal receptor with a trimethylated central benzene ring (**1a**) showed a cone-type conformation defining an inner anion-binding site, while the bipodal molecule with the central *meta*-phenylene spacer (*m*-**2a**) displayed an extended conformation. The binding properties of the chiral imidazolium hosts toward citrate, isocitrate and the two enantiomers of malate have been studied by ¹H NMR titration experiments in 9:1 CD₃CN:CD₃OH at 298.15 K. Interestingly, **1a** showed a stronger interaction with dianionic malate than with the trianionic citrate or isocitrate, suggesting that the smaller guest is better accommodated in the host cavity. Among this family, **1a** proved to be the best receptor due to a combination of a larger number of electrostatic and H-bonding interactions and to a more efficient preorganization in the cone-type conformation. This preorganization effect is also present in solution as confirmed by ¹H NMR spectroscopy.



INTRODUCTION

The study of imidazolium-containing receptors for the molecular recognition of anionic species has recently attracted much attention within the supramolecular chemistry field.¹ The unique structural characteristics of the imidazolium moiety² make this binding motif highly appealing for the interaction with anions even in competitive media. The delocalized positive charge of the ring and the high acidity of the imidazolium protons favor the establishing of C–H···anion hydrogen bonds, electrostatic contacts and anion··· π interactions. Receptors based on this scaffold have been used for the preparation of hosts, sensors and devices for halides³ and other inorganic anions,⁴ organic carboxylates⁵ and phosphates⁶ or even nucleic acids.⁷ An important issue that has been less studied is the effect of slight structural modifications on the binding abilities, especially for similar challenging substrates. Related to that, we have recently reported a robust chemoenzymatic methodology for the preparation of a large variety of enantiopure chiral imidazolium⁸ and triazolium⁹ salts. The effect of several structural variables as design vectors on their self-assembling abilities has been thoroughly studied in different media, including solution and solid states. We concluded that their properties are mainly dominated by the azolium···anion interactions, although some other secondary contacts are also important, like additional H-bonds, π – π and CH– π or

hydrophobic interactions. These weaker contributions are especially important to understand the effect of the chirality of the compounds on the supramolecular properties of the materials. Encouraged by these results, we aimed to prepare chiral enantiopure tris- and bis-imidazolium compounds (**1** and **2**, respectively, Figure 1) for assaying the molecular recognition of biologically relevant anions.¹⁰ We focused on carboxylates, since imidazolium receptors have shown to efficiently bind this functional group.¹¹ Among naturally occurring carboxylates,¹² several hydroxy-polycarboxylates are key metabolites as intermediates in the Krebs cycle.¹³ We selected citrate (**cit**), isocitrate (**isocit**) and the two enantiomers of malate (**D/L-mal**) as substrates, since they show systematic structural variations in terms of topology and stereochemistry (Figure 1) and are also important molecules in pharmaceutical, cosmetic and food industries.¹⁴

RESULTS AND DISCUSSION

Synthesis of the Bis- and Tris-Imidazolium Compounds. The synthesis of the bi- and tripodal imidazolium compounds was carried out (Scheme 1) by heating a mixture of an excess of the enantiopure alcohol **3** ((1*S*,2*S*)-2-(1-*H*-

Received: July 7, 2014

Published: September 3, 2014

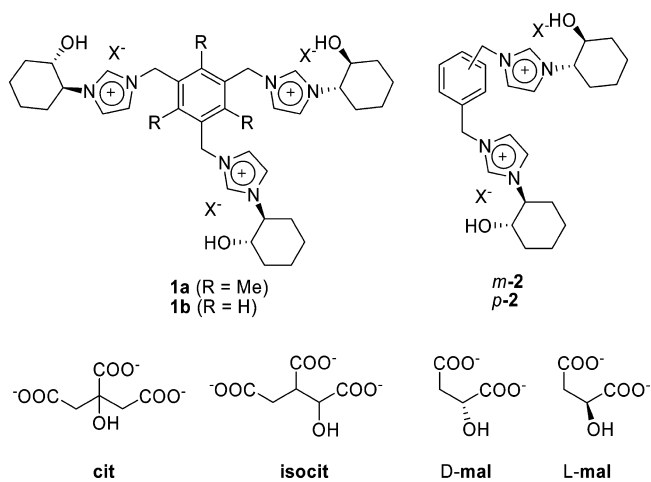
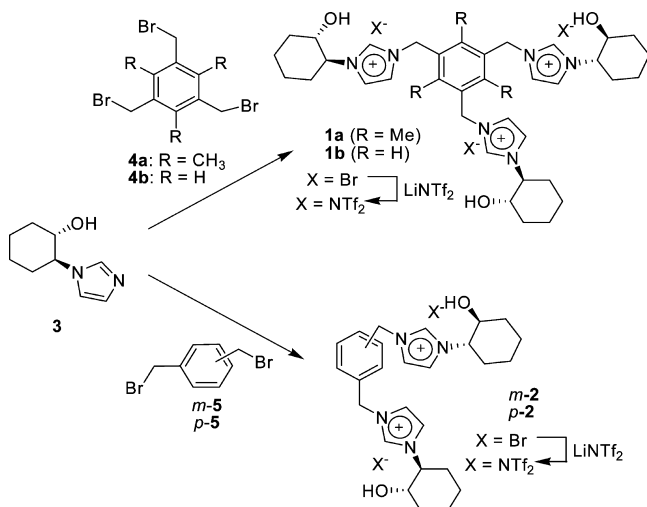


Figure 1. Chemical structures of the imidazolium receptors (1 and 2) and the polycarboxylate substrates studied in this work.

Scheme 1. Synthesis of the Tripodal (1a, 1b) and Bipodal (m-2, p-2) Chiral Imidazolium Salts



imidazol-1-yl)cyclohexanol)¹⁵ with the corresponding alkylating agent (1,3,5-tris(bromomethyl)-2,4,6-trimethylbenzene (4a), 1,3,5-tris(bromomethyl)benzene (4b), 1,3-bis(bromomethyl)benzene (m-5) or 1,4-bis(bromomethyl)benzene (p-5)) in acetonitrile (0.2 M) under microwave irradiation (150 °C, 120 W). After 20 min at the reaction temperature, the mixture was cooled down at room temperature, the solvent was decanted and the solid was washed with Et₂O to remove the excess of 3, leading to the corresponding pure product in high yield (>90%). Bi- and tripodal imidazolium salts were obtained with bromide (X = Br) as the counterion, which can be efficiently exchanged by a softer anion such as bis-(trifluoromethane) sulfonimide (X = NTf₂). The anion exchange is confirmed by the presence of a characteristic signal for the counterion found in ¹⁹F-NMR as well as by the upfield shift showed for the proton of the C2 of the imidazolium in ¹H NMR. For instance, for the tripodal compound 1b this signal shifted from 9.14 ppm for [1b·3Br] to 8.68 ppm for [1b·3NTf₂] (in CD₃OD, 500 MHz, 303 K). A similar trend was found for the anion exchange of all the imidazolium salts.

Structural Characterization of the Bromide Salts in the Solid State. Crystals suitable for X-ray diffraction analysis

were obtained by slow diffusion of acetonitrile in a methanol solution of [1a-3Br] (Figure 2). The unit cell contained two

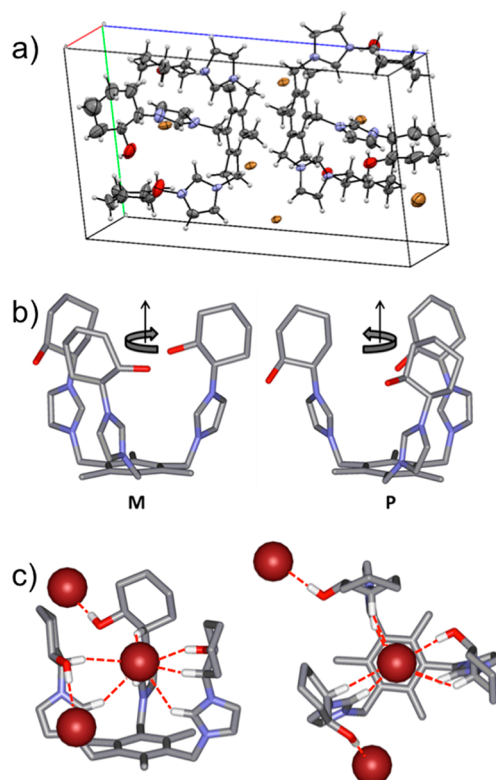


Figure 2. X-ray diffraction results for the [1a-3Br] salt: (a) Ortep representation of the crystal cell. (b) M and P helical conformations found in the crystal structure (bromide anions and H atoms omitted for clarity). (c) Detail of one of the conformers (side and up views) found in the solid state with the closer bromide anions. In (c) only the hydrogen atoms interacting with the considered bromides are shown (with H-bonds as red dashed lines).

molecules of the tris-imidazolium 1a and six bromide anions. The two molecules of the cationic receptor showed very similar (although not identical) conformations in the solid state. They both had a concave shape by setting the three imidazolium arms toward the same side of the central trimethylbenzene ring (cone-type conformation). These three arms are slightly deviated from the perpendicular to the trimethylbenzene ring plane, forming a twisted conformation with respect to the central axis. The two observed different conformers correspond to the P and M helical dispositions of the arms respectively (Figure 2b). These conformations are stabilized by specific cation–anion interactions (Figure 2c). The trication 1a shows close interactions with three bromide anions: one of them is located in the inner cavity of the concave surface of the host and the other two bromides are externally bound. The included bromide is coordinated by a network of H-bonds implicating one OH from one of the cyclohexanol moieties (OH⋯Br distance = 2.45 and 2.47 Å) and the three imidazolium cations. The interactions between the three imidazoliums and the inner bromide are established through the corresponding C2–H protons of the imidazolium rings (C2H⋯Br distance = 2.80–3.11 Å) and the three C*–H of the methynes of the cyclohexane rings close to the nitrogen atoms of the imidazoliums (C*H⋯Br distance = 2.79–3.20 Å). These hydrogens are also acidic and usually set nonconventional C–H⋯X hydrogen bonds.

Overall, the three imidazolium arms efficiently wrap the inner bromide with a tight H-bonding and electrostatic coordination sphere. The other two anions bind to **1a** through OH \cdots Br H-bonds (OH \cdots Br distance = 2.39–2.42 Å), while for one of them, an additional anion–cationic π contact can be established with one of the imidazolium cations (centroid of the imidazolium \cdots Br distance = 3.42 Å). These data identify the key interactions for the host **1a** to act as a receptor for anionic species and suggests the possibility of the simultaneous binding of the three imidazolium arms in a cone-shaped concave conformation.

We also obtained crystals suitable for X-ray diffraction of the bromide salt of *m*-2 by vapor diffusion of tBuOMe into a solution of *m*-2 in MeOH. The compound showed a completely extended conformation in the solid state, with several anion–cation interactions implicating the OH and imidazolium ring of different molecules in a compact crystal packing network (Figure 3a). The linear shape of the *m*-2

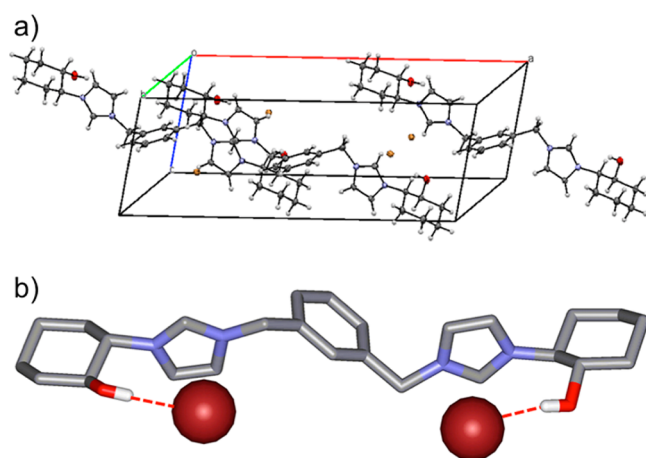


Figure 3. Plots of the crystal structure of the [*m*-2·2Br] salt: (a) crystal cell and (b) molecule view. In (b) only the hydrogen atoms interacting with the considered bromides are shown (with H-bonds as red dashed lines).

molecule displays a C_2 -symmetric geometry with two identical binding sites for the bromide anions. Each bromide sets a hydrogen bond with the hydroxyl hydrogen (OH \cdots Br distance = 2.53 Å) and an anion–cationic π interaction with the imidazolium ring (centroid of the imidazolium \cdots Br distance = 3.49 Å). The conformation and specific interactions found in the solid state for this salt suggested that this bipodal receptor could be less preorganized than the tris-imidazolium receptor (**1a**) to establish cooperative interactions with a potential polyanionic substrate.

Molecular Recognition Studies. The binding between the chiral imidazolium receptors and the carboxylate substrates was studied by ^1H NMR titration experiments at 298.15 K. We used bis(trifluoromethane) sulfonimide (NTf_2) as the anion for the imidazolium compounds and tetrabutylammonium (TBA) counterions for the carboxylate substrates. After several preliminary experiments, we found the (9:1) $\text{CD}_3\text{CN}:\text{CD}_3\text{OH}$ mixture a suitable medium for the experiments, since it renders a good solubility of the species and a suitable range for the values of the corresponding binding constants to be studied by NMR at mM concentrations.¹⁶ This polar and protic medium is rather competitive for supramolecular complexes stabilized by electrostatic and H-bonding interactions. The use of the

CD_3OH solvent is important because when we performed the titration with the more conventional CD_3OD , we observed the H/D exchange of the C2H of the imidazolium ring, thus leading to the loss of the ^1H NMR signal more affected by the coordination of the anionic substrates. Another important factor to be considered is the presence of the corresponding counterions.¹⁷ The effect of ion-pairing has been a matter of debate¹⁸ and strongly depends on the nature of the ionic species and on the polarity of the medium. Ion-pairing effects can be safely overruled in two extreme situations: (1) very polar solvents where the ions are fully solvated (and thus, ion pairs are fully dissociated) or (2) nonpolar organic solvents where the ions are 100% paired for all the considered species. In order to determine its importance in our systems, we assayed different titration procedures for the **1a**/cit host–guest system. First, we carried out the experiments by adding the substrate (cit as the TBA salt) to a solution of the receptor (**1a** as the NTf_2 salt) and keeping constant the concentration of **1a** (direct mode). Complementarily, we performed the same experiment in the reverse way, by adding **1a**·3 NTf_2 to a solution of cit 3TBA (inverse mode). The variations of several ^1H NMR signals were monitored during the titration experiments. In this way, two alternative sets of titration curves were generated. We fitted the experimental chemical shift variations of all the available signals of the two different data sets simultaneously, showing a good fit to a 1:1 binding mode (entry 1 in Table 1).

Table 1. Binding Constants Obtained by ^1H NMR Titration at 298.15 K (500 MHz, 9:1 $\text{CD}_3\text{CN}:\text{CD}_3\text{OH}$)

entry	receptor ^a	substrate ^b	log β	K_{ass} (M^{-1})
1	1a	cit	3.69 (5)	$(4.9 \pm 0.5) \times 10^3$
2	1a ^c	cit ^c	3.68 (7)	$(4.8 \pm 0.8) \times 10^3$
3	1a	isocit ^d	3.59 (5)	$(3.9 \pm 0.5) \times 10^3$
4	1a	L-mal	4.24 (7)	$(1.7 \pm 0.3) \times 10^4$
5	1a	D-mal	4.05 (7)	$(1.1 \pm 0.2) \times 10^4$
6	1b	cit	2.68 (5) ^e	480 ± 60 ^e
7	1b	L-mal	~ 3.8 ^e	$\sim 6.3 \times 10^{3e}$
8	1b	D-mal	~ 3.8 ^e	$\sim 6.3 \times 10^{3e}$
9	<i>m</i> -2	cit	3.45 (4)	$(2.8 \pm 0.2) \times 10^3$
10	<i>p</i> -2	cit	3.42 (6)	$(2.6 \pm 0.4) \times 10^3$
11	<i>m</i> -2	L-mal	3.53 (5)	$(3.4 \pm 0.4) \times 10^3$
12	<i>m</i> -2	D-mal	3.42 (5)	$(2.6 \pm 0.3) \times 10^3$

^aAs the bis(triflamide) salt. ^bAs the tetrabutylammonium salt. ^cObtained by self-dilution titration of a previously prepared [**1**·cit] complex, thus lacking other counterions. ^dThe compound isocit was used as a racemic mixture of diastereoisomers. ^eThis value is estimated since we detected the formation of other species with different stoichiometries.

The stoichiometry of the corresponding complex was additionally confirmed by ESI mass spectrometry, which clearly showed the peak at $m/z = 847.5$ corresponding to the [**1**·cit + H]⁺ species. As an alternative titration experiment, we prepared the corresponding [**1a**·cit] salt, and isolated it free of the previous counterions (TBA or NTf_2 , as confirmed by ^1H and ^{19}F NMR). This salt was dissolved in the same solvent mixture and placed in an NMR tube, and the ^1H NMR spectra were acquired at different overall concentrations (concentration range: 0.0225–11.3 mM) showing changes of representative ^1H NMR signals (self-dilution mode). These changes were also successfully fitted to a 1:1 binding mode, rendering an identical value within the experimental error (entry 2 in Table 1) than

with the other titration methods, in a very good internal consistency. The fact that different titration procedures were successfully fitted to the 1:1 model and rendered equal results confirmed the accuracy of our approach and that ion-pairing effects can be overruled in our systems. However, since the self-dilution mode requires the previous preparation and isolation of each supramolecular complex, we decided to perform the experiments in the direct or inverse mode for practical reasons. The signals more affected during the titration experiments were the imidazolium protons (especially C2H) and the proton of the cyclohexane moiety at the chiral center in α to the imidazolium nitrogen. Interestingly, these were the hydrogen atoms showing the closest contacts with the included bromide anion in the crystal structure of [1a·3Br] suggesting a similar binding epitope. The interaction of 1a with isocitrate anion (entry 3) showed practically equal binding constants (within the experimental error) than with citrate.

Interestingly, the tripodal receptor showed a 3-fold stronger binding to the malate dianion than to the citrate trianion (entry 1 vs 4–5 in Table 1). Also in this case, the binding isotherms were accurately fitted to the 1:1 stoichiometry, and confirmed by the observation of the ESI-MS peak for the corresponding supramolecular complex at $m/z = 789.5$. Thus, the smaller dianionic malate seemed to be accommodated in the concave cavity of the receptor more efficiently than the bigger citrate (see below). Comparison of the binding constants with L/D-mal rendered a low enantioselectivity toward the L-mal enantiomer ($\Delta\Delta G = 1.1$ kJ/mol) that is, however, measurable and still significant if we consider the highly competitive medium used for the titration experiments.

With the aim of evaluating the effect of the substitution on the tripodal aromatic ring, the corresponding receptor 1b lacking the methyl residues was also studied. Very remarkably, this tris-imidazolium host showed an apparent binding constant with cit 1 order of magnitude lower than that of 1a (compare entries 6 and 1 in Table 1). This difference can be explained by a favored preorganization due to the methyl substitutions on the aromatic spacer, which forces to set the three imidazolium arms to the same side in a cone-type conformation (see below). Besides, the reported stability constant for the [1b·cit] complex was obtained by fitting the NMR titration data to the simplest 1:1 stoichiometry. However, a more detailed analysis of the titration experiments suggested the participation of species of more complex stoichiometries, in equilibrium with the 1:1 complex (Supporting Information). This proposal is also supported by the observation of a slight turbidity during the titration experiments with 1b. We also performed the titration experiments with 1b and D/L-mal, rendering even more complex titration isotherms that were impossible to acceptably fit to the 1:1 binding model (the rough estimations of the binding constants for the 1:1 complexes are given in entries 7 and 8, see Supporting Information). Although the values of the binding constants for 1b must be cautiously taken, the observed trends allowed us to conclude that in the case of 1b the cationic arms are more flexible and rendered a less favored and selective binding of the polycarboxylate substrates, thus leading to the formation of more complex and nonspecific aggregates implicating several molecules of both host and guest.

We also studied the binding properties of the bipodal bis(imidazolium) receptors. In general, they behaved as less efficient hosts than 1a for all the tested substrates (Table 1, entries 9–12). Within the bipodal family, the relative position of the imidazolium groups in the central aromatic ring has no

effect on the interaction (entries 9–10 in Table 1), suggesting an inefficient host–guest complementarity. This is also reflected in a very low stereoselectivity of *m*-2 toward D/L-mal. The better host capabilities of 1a are reflected by comparing the binding of L-mal (entries 4 and 11 in Table 1) where a stronger interaction was observed for the tricationic receptor ($K_{\text{ass}}(1a + L\text{-mal})/K_{\text{ass}}(m\text{-}2 + L\text{-mal}) = 5.13$). This fact can be due to the larger positive charge of 1a and, more importantly, to its more efficient preorganization, as observed in the corresponding solid state structures (and also in solution, see below).

An interesting general observation throughout most of the titration experiments was an increase of the anisochrony of the diastereotopic benzylic methylenes of the receptors upon the addition of the guests. This effect must be related to a decrease of the flexibility of the chiral arms of the hosts upon binding that produces a more efficient transference of the chirality. The somehow more defined and chiral nature of the supramolecular structures suggests a process of induced fit of the hosts upon binding.

In order to explain the apparently different preorganization of the receptors in solution,¹⁹ we compared the ¹H NMR spectra of the hosts as the NTf₂ salts in 9:1 CD₃CN:CD₃OH at 298.15 K (Figure 4). Interestingly, the chemical shifts of

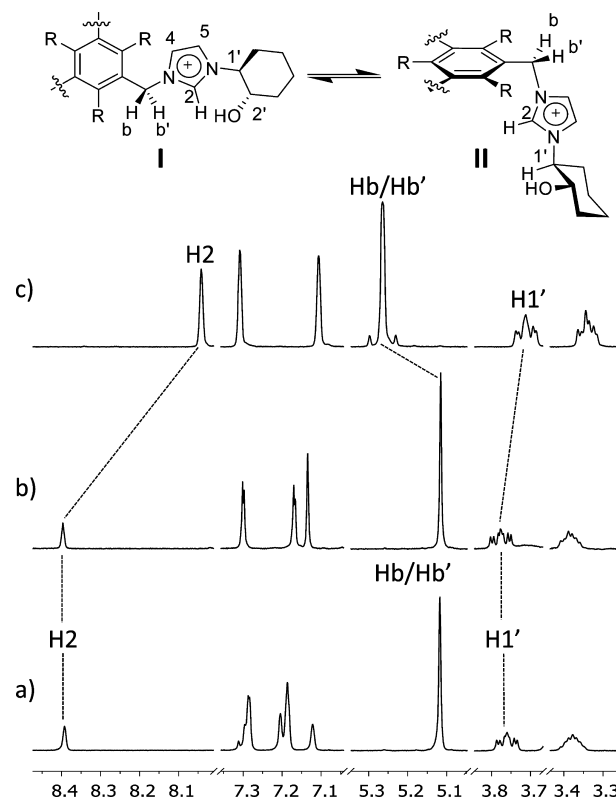


Figure 4. Partial ¹H NMR spectra (500 MHz, at 298.15 K in 9:1 CD₃CN:CD₃OH) of (a) *m*-2, (b) 1b and (c) 1a.

representative signals from the imidazolium arms (H2 and H1') and its link to the central aromatic core (Hb,b') are virtually identical for *m*-2 (Figure 4a) and 1b (Figure 4b), suggesting a similar chemical environment for the bipodal and the tripodal receptors lacking the methyl substitution at the aromatic ring. However, the Me-substituted tripodal host (1a) showed a remarkable upfield shielding of H2 and H1' and a downfield

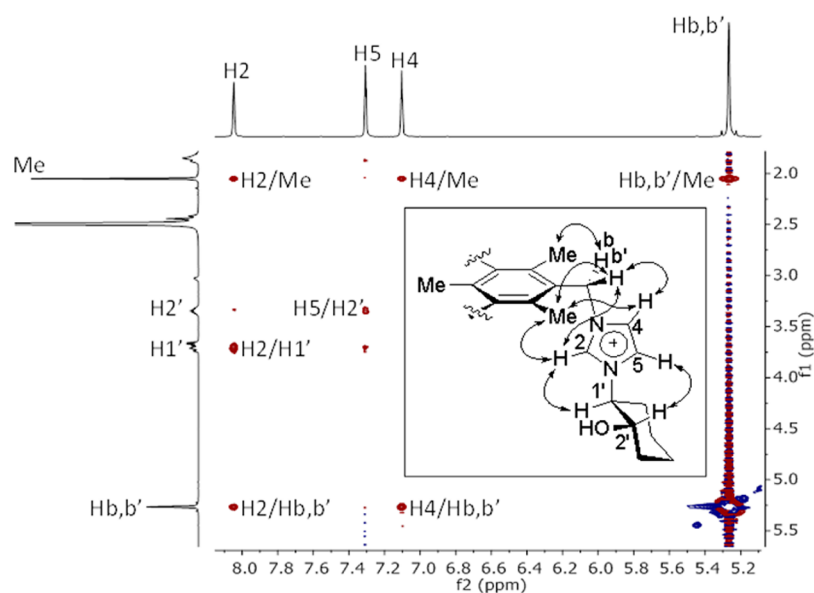


Figure 5. Selected region of the NOESY spectrum of the receptor **1a** as the tris-NTf₂ salt (400 MHz, at 298.15 K in 9:1 CD₃CN:CD₃OH). The key NOE peaks have been assigned in the spectrum and shown in the inset structure with double-headed arrows.

shift of the Hb,b' proton signals (Figure 4c). These changes can be rationalized by the rotation of the arms with respect to the central aromatic ring, as depicted in Figure 4. For **1a**, the system would be shifted to the **II** conformation, where the anisotropy of the aromatic ring would shield H2 and H1', but it would deshield Hb,b' protons. However, for *m*-**2** and **1b**, the arms are more flexible, rendering an averaged similar chemical environment. This difference is also reflected in the multiplicity of the diastereotopic Hb,b' methylenes, which appeared as a singlet for both *m*-**2** and **1b**, while as an AB quartet for **1a**.

The existence of the **II** conformation of **1a** in solution was additionally supported by a NOESY experiment (Figure 5). We observed strong NOE effects between the protons of the imidazolium ring (H2 and H4), the benzylic methylene (Hb,b') and the methyl attached to the central benzene (Me), supporting the proposed folding of the imidazolium arm. Moreover, a very strong NOE between H2 (of the imidazolium) and H1' (of the cyclohexane) protons support their *syn* disposition, as observed in the crystal structure of [**1a**·3Br]. This disposition was also confirmed by the strong NOE between H5 and H2'. Interestingly, the same NOESY experiment performed with **1b** only showed weak and trivial NOE correlations between contiguous protons (Supporting Information). Overall, all the NMR data strongly supported the existence of a preorganized cone-type conformation in solution for **1a**, but a more flexible open conformation for the other receptors. This preorganization effect nicely explains the better performance of **1a** as a host for the di- and tricarboxylate anions.

We additionally carried out simple molecular modeling calculations to try to illustrate the structural factors explaining the experimental data. Considering the experimental results, we decided to focus on the best host (**1a**) and its corresponding supramolecular complexes with cit and D/L-mal. Since the supramolecular complexes can display certain flexibility in solution, we subjected the corresponding host-guest structures to Monte Carlo conformational searches without restrictions followed by MMFF minimizations, in order to fully map all the possible conformations and anion-cation relative dispositions.

The obtained minima were subsequently optimized by DFT quantum mechanics calculations, being the corresponding global minima shown in Figure 6. For all the structures, the receptor adopts a cone-type conformation with the hydroxycarboxylate substrates included within the concave inner cavity formed by the three cationic arms. This geometry is stabilized by a number of electrostatic H-bonds between the carboxylate anions and the polar hydrogens of the receptor. These mainly implicate the hydroxyl OH groups, the imidazolium H2 and the methynes of the cyclohexane moieties in α to the imidazolium ring (H1'). Interestingly, these hydrogens were also those H-bond in the crystal structure of the bromide salt of **1a**. Besides, they also correlate with the ¹H NMR signals more shifted during the titration experiments.

The comparison of the modeled structures also gave some clues for the structural explanation of the differences observed in the stabilities of the supramolecular complexes with **1a**. First of all, the largest differences were found between the citrate and the malate complexes. The bigger citrate anion showed a less favored fit, represented by a lower number of host-guest contacts and a slight distortion of the cone conformation. The inclusion of the citrate within the host cavity forces one of the arms to move outward, as shown in Figure 6a. The interaction of this arm with the substrate occurs through the C5H hydrogen of the imidazolium ring (instead of the more acidic C2H). This could explain the lower binding constant with citrate, in spite of its larger negative charge.

The optimized geometries of the complexes of **1a** with the two enantiomers of malate were also illustrative (Figure 6b,c). Both minima showed very similar conformations with a comparable number, geometry and connectivity of H-bonds implicating the carboxylate anions of the guests (for an overlay of the two optimized geometries, see the Supporting Information). Rather reasonably, the main difference was observed in the disposition and interactions of the hydroxyl alcohol of the malate. In the L enantiomer, the malate hydroxyl is pointing to the host, possibly establishing a C*H...O H-bond with the polar methyne of the cyclohexane of one arm (Figure 6b). For the D-enantiomer, the corresponding OH is pointing

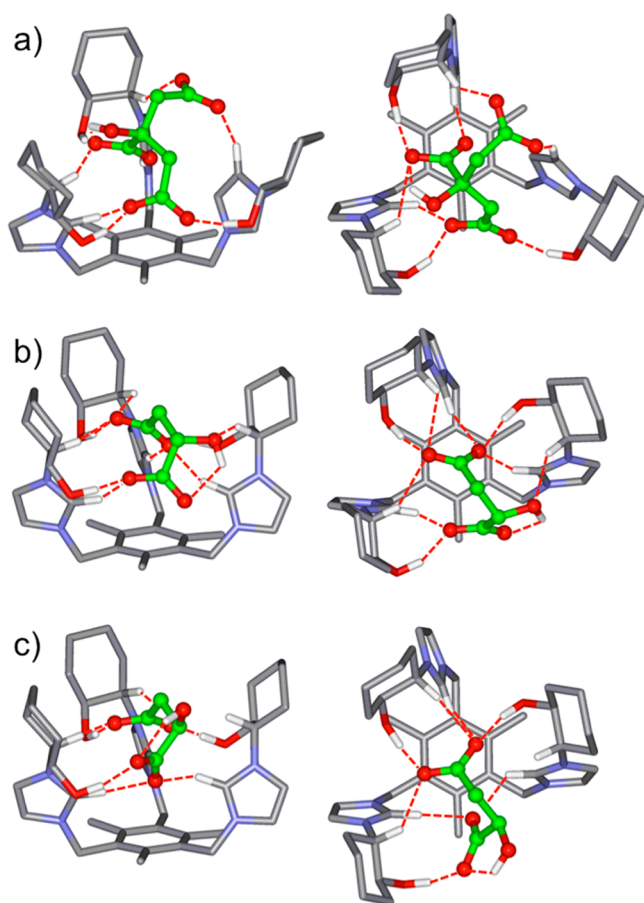


Figure 6. Global minima optimized structures for the supramolecular complexes formed between tripodal trisimidazolium **1a** and (a) *cit*, (b) *L-mal* and (c) *D-mal*. For clarity, we only show the polar hydrogens implicated in H-bonding interactions (shown as red dashed lines). The corresponding substrates are shown as ball and stick models with the C atoms in bright green.

away (Figure 6c), thus precluding any interaction with the host. This could account for the moderate *L*-selectivity exhibited by **1a**.

In order to validate the theoretical calculations, we also compared the optimized geometries of the host molecule (**1a**) in the different complexes with those experimentally observed in the crystals of [**1a**·3Br]. All the structures showed a cone-type conformation highlighting the preorganized nature of the tripodal receptor. The three optimized geometries displayed a *P*-helicity, among the two dispositions found in the solid state. Very gratifyingly, the *P*-form of the crystals overlay reasonably well with all the geometries obtained by theoretical calculations. The align factors follow the series *L-mal* (0.82) > *D-mal* (0.80) > *cit* (0.69), being the same order of the binding strength. Thus, the more stable complexes correlated with the less distorted geometry, as compared with the one containing the small spherical bromide anion. Overall, we concluded that the observed selectivity was due to a combination of more efficient H-bonding interactions and lower geometrical distortion of the host from the cone conformation.

CONCLUSIONS

Here we report the synthesis and characterization of a family of chiral bis- and tris-imidazolium salts from the easily accessible enantiopure (*S,S*)-2-(1-imidazolyl)-cyclohexanol, by the linking

to a central aromatic spacer with different substitution patterns. The corresponding crystal structures of the tripodal (**1a**) and the bipodal (*m*-2) imidazolium bromides showed a more preorganized conformation of **1a** for anion binding. Thus, **1a** presented a cone-type conformation in the solid state, with a cationic binding site in the concave surface defined by the three imidazolium arms. This binding site is occupied by one bromide anion in the crystal, which interacts with both the imidazolium rings and the hydroxyl OH groups through a network of H-bonds. On the other hand, the bipodal derivative *m*-2 showed an extended and open conformation that defines two independent binding sites for two different bromides.

The synthesized chiral imidazolium molecules were studied as host for different hydroxypolycarboxylates from the Krebs cycle, such as citrate (*cit*), isocitrate (*isocit*) and both enantiomers of malate (*D/L-mal*), by ¹H NMR titrations in a competitive solvent mixture. The results rendered interesting trends. The best receptor showed to be **1a**, which has the optimal structural features for the recognition of the substrates. Thus, **1a** has a larger number of potential cationic and H-bonding donor sites, as compared with the bipodal derivatives *m/p*-2. Besides, the methyl substitutions on the central benzene ring favor the concave conformation finally making **1a** a more efficient and selective receptor for the studied anions than the flexible tris(imidazolium) **1b**. The higher degree of preorganization of **1a** versus *p/m*-2 and, specially, **1b** has been confirmed by the NMR studies of the receptors as the NTf₂ salts. Interestingly, **1a** showed a stronger interaction with the malate dianion than with the citrate/isocitrate trianion, with a modest enantioselectivity toward *L*-malate. These observations suggested that the smaller substrate (malate) fits better in the host cavity. The experimental results were also supported by theoretical calculations, reflecting that the binding efficiency/selectivity of **1a** is a result of the larger number of polar H-bonding interactions located in a suitable cavity defined by a preorganized concave conformation.

Our study with this family of imidazolium receptors is an illustrative example of the importance of the host–guest complementarity for the molecular recognition process. In our case, this complementarity is better represented by the conformational preorganization of the receptor than by the electrostatic match between the host and the guest. Thus, the tricationic **1a** binds more efficiently to the dianionic malate than to the trianionic citrate or isocitrate, because the smaller dianion fits better in the host binding cavity. Moreover, the differences observed between the two tricationic receptors **1a,b** highlight the importance of the conformational preorganization for the efficient binding, which turned out to be the key factor in these supramolecular processes.

EXPERIMENTAL SECTION

General Experimental Methods. Reagents and solvents were purchased from commercial suppliers and were used without further purification. All the microwave experiences were run in constant temperature mode. The NMR spectra were performed on spectrometers operating at 500 or 400 MHz for ¹H and 125 or 100 MHz for ¹³C NMR. The chemical shifts are reported in ppm using tetramethylsilane (TMS) as a reference. High resolution mass spectra (HRMS) were performed on an UPLC system coupled with an orthogonal acceleration time-of-flight (oa-TOF) equipped with an electrospray ionization source. Melting points were determined with a differential scanning calorimeter at the onset of the transition.

General Procedure for the Alkylation Reaction. A mixture of alcohol **3** ((*1S,2S*)-2-(1*H*-imidazol-1-yl)cyclohexanol) (2.2 equiv) and

either 1,3-bis(bromomethyl)benzene (*m*-5) or 1,4-bis(bromomethyl)benzene (*p*-5) (1 equiv) in CH₃CN (0.4 M) was heated and stirred under MW irradiation at 150 °C, in constant temperature mode (Nominal Power 120 W), during 20 min. Then the reaction mixture was cooled down to room temperature, the solvent was decanted, and the resulting solid was washed with Et₂O (5 × 10 mL) affording the corresponding pure product as a solid. When 1,3,5-tris(bromomethyl)-2,4,6-trimethylbenzene (4a) or 1,3,5-tris(bromomethyl)benzene (4b) (1 equiv) were employed, 5 equiv of the alcohol 3 ((1*S*,2*S*)-2-(1*H*-imidazol-1-yl)cyclohexanol) were used.

[1a-3Br]. White solid; 608 mg, 92% yield; mp 305.1 °C; ¹H NMR (CD₃OD, 500 MHz) δ 1.36–1.58 (m, 3H), 1.79–1.99 (m, 3H), 2.04–2.21 (m, 2H), 2.36 (s, 3H), 3.69 (td, *J* = 10.1, 4.3 Hz, 1H), 4.33 (ddd, *J* = 13.8, 10.1, 4.1 Hz, 1H), 5.63 (q, *J* = 15.4 Hz, 2H), 7.76 (t, *J* = 1.8 Hz, 1H), 7.80 (t, *J* = 1.8 Hz, 1H), 9.14 (d, *J* = 13.7 Hz, 1H); ¹³C NMR (CD₃OD, 125 MHz) δ 15.8, 23.8, 24.5, 30.8, 34.6, 48.5, 66.1, 72.3, 121.4, 123.3, 130.1, 136.5, 142.6; IR (ATR) ν 3350, 3281, 3265, 3053, 2933, 2855, 1571, 1551, 1158, 1138, 1083 cm⁻¹; HRMS (ESI-TOF) *m/z* [1a + Br]²⁺ Calcd for (C₃₉H₅₇BrN₆O₃/2) 368.1832, found 368.1829; [α]_D²⁰ = -11.59 (*c* = 0.01, MeOH).

[1b-3Br]. White solid; 426 mg, 91% yield; mp 109.8 °C; ¹H NMR (CD₃OD, 500 MHz) δ 1.37–1.55 (m, 3H), 1.76–1.99 (m), 2.05–2.26 (m, 2H), 3.71 (td, *J* = 10.0, 4.5 Hz, 1H), 4.09–4.16 (m, 1H), 5.52 (q, *J* = 15.4 Hz, 2H), 7.65 (s, 1H), 7.71 (d, *J* = 1.9 Hz, 1H), 7.75 (d, *J* = 2.0 Hz, 1H), 9.14 (d, *J* = 13.7 Hz, 1H); ¹³C NMR (CD₃OD, 125 MHz) δ 25.0, 25.7, 32.3, 35.6, 53.2, 67.6, 73.2, 122.6, 123.8, 130.9, 131.0, 137.6; IR (ATR) ν 3307, 3099, 3065, 2931, 2856, 1555, 1158, 1141, 1072 cm⁻¹; HRMS (ESI-TOF) *m/z* [1b + Br]²⁺ Calcd for (C₃₆H₅₁BrN₆O₃/2) 347.1597, found 347.1600; [α]_D²⁰ = 4.48 (*c* = 0.01, MeOH).

[*m*-2-2Br]. White solid; 661 mg, 97% yield; mp 178.6 °C; ¹H NMR (CD₃OD, 500 MHz) δ 1.38–1.56 (m, 3H), 1.78–1.98 (m, 3H), 2.04–2.23 (m, 2H), 3.70 (td, *J* = 9.9, 4.5 Hz, 1H), 4.10 (ddd, *J* = 12.4, 10.0, 4.0 Hz, 1H), 5.50 (s, 2H), 7.46–7.57 (m, 2H), 7.65 (s, 1H), 7.68 (d, *J* = 2.0 Hz, 1H), 7.76 (d, *J* = 2.0 Hz, 1H), 9.24 (s, 1H); ¹³C NMR (CD₃OD, 125 MHz) δ 24.8, 25.5, 32.2, 35.5, 53.6, 67.7, 73.3, 123.2, 124.1, 130.7, 131.1, 131.9, 137.0, 137.6; IR (ATR) ν 3290, 3069, 2924, 2855, 1554, 1165, 1068, cm⁻¹; HRMS (ESI-TOF) *m/z* [*m*-2]²⁺ Calcd for (C₂₆H₃₆N₄O₂/2) 218.1413, found 218.1415; [α]_D²⁰ = 17.72 (*c* = 0.01, MeOH).

[*p*-2-2Br]. White solid; 624 mg, 92% yield; mp 240.8 °C; ¹H NMR (CD₃OD, 500 MHz) δ 1.38–1.56 (m, 3H), 1.77–1.98 (m, 3H), 2.08–2.19 (m, 2H), 3.68 (td, *J* = 9.9, 4.6 Hz, 1H), 4.08 (ddd, *J* = 13.9, 10.1, 4.1 Hz, 1H), 5.48 (s, 2H), 7.52 (s, 2H), 7.64 (d, *J* = 2.0 Hz, 1H), 7.76 (d, *J* = 2.0 Hz, 1H), 9.19 (s, 1H); ¹³C NMR (CD₃OD, 125 MHz) δ 24.9, 25.7, 32.3, 35.6, 53.5, 67.7, 73.2, 122.8, 123.7, 130.5, 130.8, 136.4, 137.2; IR (ATR) ν 3327, 3123, 3064, 2927, 2855, 1556, 1419, 1159, 1073 cm⁻¹; HRMS (ESI-TOF) *m/z* [*p*-2]²⁺ Calcd for (C₂₆H₃₆N₄O₂/2) 218.1413, found 218.1419; [α]_D²⁰ = 11.92 (*c* = 0.01, MeOH).

General Procedure for the Anion Exchange. A solution of lithium bis(trifluoromethane) sulfonimide (3.2 equiv) in H₂O (0.55 M) was added to a solution of the tris-imidazolium bromide salt (1 equiv) in MeOH (0.02 M). The resulting solution was stirred during 24 h at room temperature. Then MeOH was evaporated at reduced pressure, and ethyl acetate (20 mL) was added. The organic phase was washed with H₂O (3 × 10 mL), dried over Na₂SO₄, and the solvent was evaporated under reduced pressure affording the corresponding bis(trifluoromethane) sulfonimide salt. For the anion exchange of bis-imidazolium bromide salts, 2.2 equiv of lithium bis(trifluoromethane) sulfonimide were used.

[1a-3NTf₂]. White solid; 228 mg, 90% yield; ¹H NMR (CD₃OD, 500 MHz) δ 1.33–1.54 (m, 3H), 1.74–1.96 (m, 3H), 2.06–2.19 (m, 2H), 2.38 (s, 3H), 3.55–3.68 (m, 1H), 3.95–4.11 (m, 1H), 5.64 (q, *J* = 15.4 Hz, 2H), 7.51 (d, *J* = 1.8 Hz, 1H), 7.75 (d, *J* = 1.8 Hz, 1H), 8.68 (s, 1H); ¹⁹F NMR (CD₃OD, 470 MHz) δ 80.5; IR (ATR) ν 3506, 3147, 2947, 2868, 1349, 1325, 1178, 1130, 1053, cm⁻¹; HRMS (ESI-TOF) *m/z* [1a + NTf₂]²⁺ Calcd for (C₄₁H₅₇F₆N₇O₇S₂/2) 468.6824, found 468.6828.

[1b-3NTf₂]. Colorless viscous liquid; 77.6 mg, 90% yield; ¹H NMR (CD₃OD, 500 MHz) δ 1.37–1.52 (m, 3H), 1.75–1.97 (m, 3H), 2.07–2.26 (m, 2H), 3.67 (dd, *J* = 12.1, 7.8 Hz, 1H), 4.00–4.11 (m, 1H),

5.47 (s, 2H), 7.48 (s, 1H), 7.58 (d, *J* = 1.8 Hz, 1H), 7.75 (d, *J* = 1.8 Hz, 1H), 8.95 (s, 1H); ¹⁹F NMR (CD₃OD, 470 MHz) δ 80.6; IR (ATR) ν 3525, 3151, 2947, 2869, 1344, 1181, 1131, 1052 cm⁻¹; HRMS (ESI-TOF) *m/z* [1b + 2(NTf₂)]⁺ Calcd for C₄₀H₅₁F₁₂N₈O₁₁S₄ 1175.2352, found 1175.2415.

[*m*-2-2NTf₂]. Colorless viscous liquid; 226 mg, 90% yield; empirical formula C₃₀H₃₆F₁₂N₆O₁₀S₄; *M_w* 996.88 g/mol; ¹H NMR (CD₃OD, 500 MHz) δ 1.37–1.54 (m, 3H), 1.76–1.96 (m, 3H), 2.08–2.22 (m, 2H), 3.66 (dd, *J* = 12.2, 7.7 Hz, 1H), 3.99–4.12 (m, 1H), 5.45 (s, 2H), 7.43–7.55 (m, 3H), 7.60 (d, *J* = 1.8 Hz, 1H), 7.75 (d, *J* = 1.9 Hz, 1H); ¹⁹F NMR (CD₃OD, 470 MHz) δ 80.6; IR (ATR) ν 3524, 3147, 2946, 2868, 1345, 1180, 1131, 1051 cm⁻¹; HRMS (ESI-TOF) *m/z* [*m*-2]²⁺ Calcd for (C₂₆H₃₆N₄O₂/2) 218.1413, found 218.1412; [*m*-2 + NTf₂]⁺ Calcd for C₂₈H₃₆F₆N₅O₆S₂ 716.2000, found 716.2026.

[*p*-2-2NTf₂]. Colorless viscous liquid; 115 mg, 90% yield; ¹H NMR (CD₃OD, 500 MHz) δ 1.39–1.51 (m, 3H), 1.74–1.96 (m, 3H), 2.06–2.19 (m, 2H), 3.62–3.71 (m, 1H), 4.00–4.09 (m, 1H), 5.45 (s, 2H), 7.49 (s, 2H), 7.61 (s, 1H), 7.74 (s, 1H), 9.06 (s, 1H); ¹⁹F NMR (CD₃OD, 470 MHz) δ 80.6; IR (ATR) ν 3525, 3148, 2945, 2868, 1345, 1180, 1132, 1051 cm⁻¹; HRMS (ESI-TOF) *m/z* [*p*-2]²⁺ Calcd for (C₂₆H₃₆N₄O₂/2) 218.1413, found 218.1417; [*p*-2 + NTf₂]⁺ Calcd for C₂₈H₃₆F₆N₅O₆S₂ 716.2000, found 716.2001.

General Procedure for the Synthesis of the Receptor-Carboxylate Complexes.

1a-3Br (20.1 mg, 0.022 mmol) was dissolved in MeOH (8 mL); to this solution was added Amberlite IRA-900 OH resin (500 mg). The mixture was shaken during 30 min and then filtered and washed several times with MeOH. To the solution containing 1a-3OH was added citric acid (4.22 mg, 0.022 mmol, 1 equiv) and the resulting solution was stirred during 30 min; solvents were evaporated at reduced pressure, affording 1a-cit as a white solid (18.6 mg, 0.022 mmol, quantitative yield).

Preparation of the TBA Salts of the Substrates. Synthesis of (TBA)₂-L-Malate. L-Malic acid (500 mg, 3.73 mmol) was dissolved in 20 mL of methanol, and to this solution was added tetrabutylammonium hydroxide 30-hydrate (5.97 g, 7.46 mmol) and the mixture was stirred at room temperature for 30 min. Solvents were evaporated at reduced pressure, affording (TBA)₂-L-malate as a pale yellow thick oil (2.29 g, 3.73 mmol, quantitative yield): ¹H NMR (CDCl₃, 400 MHz) δ 4.15 (d, *J* = 7.1 Hz, 1H), 3.21–3.17 (m, 16H), 2.63 (dd, *J* = 14.7, 2.7 Hz, 1H), 2.15 (dd, *J* = 14.7, 9.8 Hz, 1H), 1.59–1.51 (m, 16H), 1.39–1.30 (m, 16H), 0.90 (t, *J* = 7.3 Hz, 24H). For the D-malate substrate, we followed exactly the same experimental procedure using D-malic acid and yielding the same spectral data.

Synthesis of (TBA)₃-Citrate. Citric acid (500 mg, 2.60 mmol) was dissolved in 20 mL of methanol, and to this solution was added tetrabutylammonium hydroxide 30-hydrate (6.25 g, 7.81 mmol), and the mixture was stirred at room temperature for 30 min. Solvents were evaporated at reduced pressure, affording (TBA)₃-citrate as a pale yellow thick oil (2.38 g, 2.60 mmol, quantitative yield): ¹H NMR (CDCl₃, 400 MHz) δ 3.31–3.26 (m, 24H), 2.68 (ABq, 4H, Δδ_{AB} = 0.03, *J*_{AB} = 14.9 Hz), 1.67–1.59 (m, 24H), 1.47–1.38 (m, 24H), 0.97 (t, *J* = 7.3 Hz, 36H).

Synthesis of (TBA)₃-Isocitrate. Isocitric acid (500 mg, 2.60 mmol) was dissolved in 20 mL of methanol, and to this solution was added tetrabutylammonium hydroxide 30-hydrate (6.25 g, 7.81 mmol), and the mixture was stirred at room temperature for 30 min. Solvents were evaporated at reduced pressure, affording (TBA)₃-isocitrate as a pale yellow thick oil (2.38 g, 2.60 mmol, quantitative yield): ¹H NMR (CDCl₃, 400 MHz) δ 4.26 (d, *J* = 3.2 Hz, 1H), 3.33–3.29 (m, 24H), 3.08 (td, *J* = 6.6, 3.2 Hz, 1H), 2.74 (dd, *J* = 16.2, 6.8 Hz, 1H), 2.57 (dd, *J* = 16.2, 6.4 Hz, 1H), 1.67–1.60 (m, 24H), 1.47–1.38 (m, 24H), 0.97 (t, *J* = 7.3 Hz, 36H).

NMR Titration Procedures. The titrations were performed with the imidazolium receptors as bis-triflamide salts. Stock solutions of the receptors were prepared by weighting the corresponding amount of the receptor and reaching a final concentration around 1–3 mM. A 9:1 CD₃CN:CD₃OH mixture was used as solvent, as it allowed good solubility of both receptors and substrates. Titrations were carried out using both the autodilution method (entry 2) and the conventional method (entries 1 and 3–12). In the first case a sample containing

equimolar amounts of imidazolium receptor and carboxylate was prepared and its ^1H NMR (400 MHz, 298 K) spectrum acquired. Then it was repeatedly diluted and its NMR spectrum acquired after each dilution. In the latter case a stock solution of the titrant containing 40 mM carboxylate was prepared by dissolving the carboxylate in the stock solution of the corresponding receptor, thus maintaining the concentration of the receptor constant during the titration experiment. The stock solution of the receptor was introduced in a NMR tube and the ^1H NMR spectrum (500 MHz, 298 K) was acquired, then volumes of the stock solution of the carboxylate were added and the ^1H NMR spectrum recorded after each addition. Different signals shifted along the titration samples, and their shifts were simultaneously fitted by multivariate analysis using the specific software (for details, see the Supporting Information).

Molecular Modeling. The supramolecular complexes between **1a** and the guests were generated manually and submitted to conformational analysis by Monte Carlo conformational searches. To this aim, 10 000 structures were stochastically generated and minimized with the MMFF molecular force field. Then, the lowest 100 minima were analyzed and ordered attending to their relative energies. Different starting geometries and anion–cation dispositions were used in order to verify that the systems converged to the same final minima. The obtained minima were subsequently fully minimized at the B3LYP/6-31+G**/B3LYP/3-21G* level of theory.

■ ASSOCIATED CONTENT

📄 Supporting Information

Further experimental details, characterization data, X-ray diffraction data, NMR titration procedures and data for the determination of K_{ass} , additional NMR spectra, molecular modeling details including Cartesian coordinates. This material is available free of charge via the Internet at <http://pubs.acs.org>.

■ AUTHOR INFORMATION

Corresponding Author

*E-mail: ignacio.alfonso@iqac.csic.es.

Notes

The authors declare no competing financial interest.

■ ACKNOWLEDGMENTS

This work was supported by the Spanish Ministry of Economy and Competitiveness (MINECO, CTQ2012-38543-C03 and CTQ 2011-28903-C02-01 projects), GV (PROMETEO/2012/020) and Pla de Promoció de la Investigació de la Universitat Jaume I (P1-1B2013-37). E.F. also thanks CSIC and the European Social Fund for personal financial support (JAE-doc program).

■ REFERENCES

- (1) (a) Yoon, J.; Kim, S. K.; Singh, N. J.; Kim, K. S. *Chem. Soc. Rev.* **2006**, *35*, 355. (b) Xu, Z.; Kim, S. K.; Yoon, J. *Chem. Soc. Rev.* **2010**, *39*, 1457 and references cited therein. (c) D'Anna, F.; Noto, R. *Eur. J. Org. Chem.* **2014**, 4201.
- (2) Mercsa, L.; Albrecht, M. *Chem. Soc. Rev.* **2010**, *39*, 1903.
- (b) Noujeim, N.; Leclercq, L.; Schmitzer, A. R. *Curr. Org. Chem.* **2010**, *17*, 1500. (c) Riduan, S. N.; Zhang, Y. *Chem. Soc. Rev.* **2013**, *42*, 9055.
- (3) (a) Bollough, E. K.; Kilner, C. A.; Little, M. A.; Willans, C. E. *Org. Biomol. Chem.* **2012**, *10*, 2824. (b) Do-Thanh, C.-L.; Khanal, N.; Lu, Z.; Cramer, S. A.; Jenkins, D. M.; Best, M. D. *Tetrahedron* **2012**, *68*, 1669. (c) Jun, E. J.; Xu, Z.; Lee, M.; Yoon, J. *Tetrahedron Lett.* **2013**, *54*, 2755. (d) Mashraqui, S. H.; Betkar, R.; Chandiramani, M.; Quinero, D.; Frontera, A. *Tetrahedron Lett.* **2010**, *51*, 596. (e) Su, Z.-M.; Ye, H.-M.; Zhu, X.-X.; Xie, L.-L.; Bai, S.; Yuan, Y.-F. *J. Organomet. Chem.* **2014**, *750*, 162. (f) Suresh, V.; Ahmed, N.; Youn, I. S.; Kim, K. S. *Chem.—Asian J.* **2012**, *7*, 658. (g) Chun, Y.; Jiten Singh, N.; Hwang, I.-C.; Woo Lee, J.; Yu, S. U.; Kim, K. S. *Nat. Commun.*

2013, *4*, 1797. (h) García, J. S.; Rodríguez, L.; Gamez, P.; Robertazzi, A. *J. Phys. Chem. A* **2012**, *116*, 9110.

(4) (a) Zhou, H.; Zhao, Y.; Gao, G.; Li, S.; Lan, J.; You, J. *J. Am. Chem. Soc.* **2013**, *135*, 14908–14911. (b) Amendola, V.; Boiocchi, M.; Colasson, B.; Fabbri, L.; Douton-Rodriguez, M.-J.; Ugozzoli, F. *Angew. Chem., Int. Ed.* **2006**, *45*, 6920.

(5) (a) Kim, S. K.; Kang, B.-G.; Koh, H. S.; Yoon, Y.-J.; Jung, S. J.; Jeong, B.; Lee, K.-D.; Yoon, J. *Org. Lett.* **2004**, *6*, 4655. (b) Koner, A. L.; Schatz, J.; Nau, W. M.; Pischel, U. *J. Org. Chem.* **2007**, *72*, 3889. (c) Yang, L.; Qin, S.; Su, X.; Yang, F.; You, J.; Hu, C.; Xie, R.; Lan, J. *Org. Biomol. Chem.* **2010**, *8*, 339. (d) Ahmad, Md. W.; Kim, S. H.; Kim, H.-S. *Tetrahedron Lett.* **2011**, *52*, 6743. (e) González, L.; Altava, B.; Bolte, M.; Burguete, M. I.; García-Verdugo, E.; Luis, S. V. *Eur. J. Org. Chem.* **2012**, 4996. (f) Roy, B.; Bar, A. K.; Gole, B.; Mukherjee, J. *Org. Chem.* **2013**, *78*, 1306. (g) Casal-Dujat, L.; Griffiths, P. C.; Rodríguez-Abreu, C.; Solans, C.; Rogers, S.; Pérez-García, L. *J. Mater. Chem. B* **2013**, *1*, 4963. (h) Wang, F.; Nandhakumar, R.; Hu, Y.; Kim, D.; Kim, K. M.; Yoon, J. *J. Org. Chem.* **2013**, *78*, 11571. (i) Lu, Q.; Hou, J.; Wang, J.; Xu, B.; Zhang, J.; Yu, X. *Chin. J. Chem.* **2013**, *31*, 641.

(6) (a) Kim, S. K.; Singh, N. J.; Kim, S. J.; Kim, H. G.; Kim, J. K.; Lee, J. W.; Kim, K. S.; Yoon, J. *Org. Lett.* **2003**, *5*, 2083. (b) Yoon, J.; Kim, S. K.; Singh, N. J.; Lee, J. W.; Yang, Y. J.; Sellappan, K.; Kim, K. S. *J. Org. Chem.* **2004**, *69*, 581. (c) Kwon, J. Y.; Singh, N. J.; Kim, H.; Kim, S. K.; Kim, K. S.; Yoon, J. *J. Am. Chem. Soc.* **2004**, *126*, 8892. (d) Xu, Z.; Singh, N. J.; Lim, J.; Pan, J.; Kim, H. N.; Park, S.; Kim, K. S.; Yoon, J. *J. Am. Chem. Soc.* **2009**, *131*, 15528. (e) Ahmed, N.; Shirinfar, B.; Geronimo, I.; Kim, K. S. *Org. Lett.* **2011**, *13*, 5476. (f) Kim, H. N.; Moon, J. H.; Kim, S. K.; Kwon, J. Y.; Jang, Y. J.; Lee, J. Y.; Yoon, J. *J. Org. Chem.* **2011**, *76*, 3805. (g) Jadhav, J. R.; Bae, C. H.; Kim, H.-S. *Tetrahedron Lett.* **2011**, *52*, 1623. (h) Jung, J. Y.; Jun, E. J.; Kwon, Y.-U.; Yoon, J. *Chem. Commun.* **2012**, *48*, 7928. (i) Wu, N.; Lan, J.; Yan, L.; You, J. *Chem. Commun.* **2014**, *50*, 4438.

(7) (a) Neelakandan, P. P.; Ramaiah, D. *Angew. Chem., Int. Ed.* **2008**, *47*, 8407. (b) Li, Q.-L.; Huang, J.; Wang, Q.; Jiang, N.; Xia, C.-Q.; Lin, H.-H.; Wu, J.; Yu, X.-Q. *Bioorg. Med. Chem.* **2006**, *14*, 4151. (c) Shirinfar, B.; Ahmed, N.; Park, Y. S.; Cho, G.-S.; Youn, I. S.; Nam, J.-K. H. G.; Kim, K. S. *J. Am. Chem. Soc.* **2013**, *135*, 90. (d) Wang, M.-Q.; Li, K.; Xu, H.-R.; Yu, X.-Q. *Anal. Methods* **2013**, *5*, 5903.

(8) (a) Busto, E.; Gotor-Fernández, V.; Ríos-Lombardía, N.; García-Verdugo, E.; Alfonso, I.; García-Granda, S.; Menéndez-Velázquez, A.; Burguete, M. I.; Luis, S. V.; Gotor, V. *Tetrahedron Lett.* **2007**, *48*, 5251. (b) Ríos-Lombardía, N.; Busto, E.; Gotor-Fernández, V.; Gotor, V.; Porcar, R.; García-Verdugo, E.; Luis, S. V.; Alfonso, I.; García-Granda, S.; Menéndez-Velázquez, A. *Chem.—Eur. J.* **2010**, *16*, 836.

(9) Porcar, R.; Ríos-Lombardía, N.; Busto, E.; Gotor-Fernández, V.; Montejo-Bernardo, J.; García-Granda, S.; Luis, S. V.; Gotor, V.; Alfonso, I.; García-Verdugo, E. *Chem.—Eur. J.* **2013**, *19*, 892.

(10) (a) Sessler, J. L.; Gale, P. A.; Cho, W. S. *Anion Receptor Chemistry*; RSC Publishing: Cambridge, 2006. (b) Special Issue: Anion Coordination Chemistry II, Lever, A. B. P.; Gale, P. A., Eds.; *Coord. Chem. Rev.* **2006**, *250*, 2917. (c) Kubik, S. Receptors for Biologically Relevant Anions. In *Anion Coordination Chemistry*; Bowman-James, K.; Bianchi, A.; García-España, E., Eds.; Wiley-VCH: Weinheim, Germany, 2011.

(11) Marullo, S.; D'Anna, F.; Cascino, M.; Noto, R. *J. Org. Chem.* **2013**, *78*, 10203.

(12) (a) Metzger, A.; Lynch, V. M.; Anslyn, E. V. *Angew. Chem., Int. Ed.* **1997**, *36*, 862. (b) Metzger, A.; Anslyn, E. V. *Angew. Chem., Int. Ed.* **1998**, *37*, 649. (c) Clares, M. P.; Lodeiro, C.; Fernández, D.; Parola, A. J.; Pina, F.; García-España, E.; Soriano, C.; Tejero, R. *Chem. Commun.* **2006**, 3824. (d) Schmuck, C.; Schwegmann, M. *Org. Biomol. Chem.* **2006**, *4*, 836. (e) Swinburne, A. N.; Paterson, M. J.; Fischer, K. H.; Dickson, S. J.; Wallace, E. V. B.; Belcher, W. J.; Beeby, A.; Steed, J. W. *Chem.—Eur. J.* **2010**, *16*, 1480. (f) Vajpayee, V.; Song, Y. H.; Lee, M. H.; Kim, H.; Wang, M.; Stang, P. J.; Chi, K.-W. *Chem.—Eur. J.* **2011**, *17*, 7837. (g) Wang, Q.-Q.; Day, V. W.; Bowman-James, K. *Chem. Sci.* **2011**, *2*, 1735. (h) Haynes, C. J. E.; Berry, S. N.; Garric, J.; Herniman,

J.; Hiscock, J. R.; Kirby, I. L.; Light, M. E.; Perkes, G.; Gale, P. A. *Chem. Commun.* **2013**, 49, 246.

(13) (a) Stryer, L.; Berg, J. M.; Tymoczko, J. L. *Biochemistry*, 5th ed.; W. H. Freeman: New York, 2002. (b) Newsholme, P.; Brennan, L.; Bender, K. *Diabetes* **2006**, 55, S39. (c) Satrústegui, J.; Contreras, L.; Ramos, M.; Marmol, P.; del Arco, A.; Saheki, T.; Pardo, B. *J. Neurosci. Res.* **2007**, 85, 3359. (d) Nielsen, T. T.; Stottrup, N. B.; Lofgren, B.; Botker, H. E. *Cardiovasc. Res.* **2011**, 91, 382.

(14) *Wiley Encyclopedia of Food Science and Technology*, 2nd ed.; Francis, F. J., Ed.; Wiley-VCH: Weinheim, Germany, 1999.

(15) Porcar, R.; Sans, V.; Ríos-Lombardía, N.; Gotor-Fernández, V.; Gotor, V.; Burguete, M. I.; García-Verdugo, E.; Luis, S. V. *ACS Catal.* **2012**, 2, 1976.

(16) (a) Fielding, L. *Tetrahedron* **2000**, 56, 6151. (b) Hirose, K. *J. Inclusion Phenom.* **2001**, 39, 193. (c) Hirose, K. Determination of Binding Constants. In *Analytical Methods in Supramolecular Chemistry*; Schalley, C. A., Ed.; Wiley-VCH: Weinheim, Germany, 2007. (d) Thordarson, P. *Chem. Soc. Rev.* **2011**, 40, 1305. (e) García, J.; Martins, L. G.; Pons, M. NMR Spectroscopy in Solution. In *Supramolecular Chemistry: From Molecules to Nanomaterials*; Gale, P. A., Steed, J. W., Eds.; Wiley: New York, 2012.

(17) (a) Jones, J. W.; Gibson, H. W. *J. Am. Chem. Soc.* **2003**, 125, 7001. (b) Huang, F.; Jones, J. W.; Slebodnick, C.; Gibson, H. W. *J. Am. Chem. Soc.* **2003**, 125, 14458. (c) Roelens, S.; Vacca, A.; Venturi, C. *Chem.—Eur. J.* **2009**, 15, 2635. (d) Francisco, V.; Basilio, N.; García-Río, L. *J. Phys. Chem. B* **2012**, 116, 5308.

(18) (a) Roelens, S.; Vacca, A.; Francesconi, O.; Venturi, C. *Chem.—Eur. J.* **2009**, 15, 8296. (b) Howe, E. N. W.; Bhadbhade, M.; Thordarson, P. *J. Am. Chem. Soc.* **2014**, 136, 7505.

(19) (a) Davis, A. P.; Perry, J. J.; Williams, R. P. *J. Am. Chem. Soc.* **1997**, 119, 1793. (b) Hettche, F.; Reiß, P.; Hoffmann, R. H. *Chem.—Eur. J.* **2002**, 8, 4946. (c) Ihm, H.; Yun, S.; Kim, H. G.; Kim, J. K.; Kim, K. S. *Org. Lett.* **2002**, 4, 2897.